



**Rapid Induction of Neuronal Phenotypes in Mesenchymal Stem Cells: A Morphological Observation**

Journal:	<i>Malaysian Journal of Medicine &amp; Health Sciences</i>
Manuscript ID	MJMHS-2025-1590
Manuscript Type:	Original Article
Keywords:	mesenchymal stem cells, neurogenic differentiation, small molecules, $\beta$ -mercaptoethanol, neuronal morphology

SCHOLARONE™  
Manuscripts

## ABSTRACT

**Introduction:** The restricted regenerative potential of the central nervous system remains a significant barrier in the treatment of neurodegenerative disorders such as Alzheimer's and Parkinson's diseases. Mesenchymal stem cells (MSCs) offer a promising therapeutic avenue due to their multipotency and ability to differentiate into neuronal phenotypes. This study evaluated the neurogenic potential of  $\beta$ -mercaptoethanol (BME), a low-cost thiol-based small molecule, by morphological assessment post-treatment of bone marrow-derived MSCs with BME.

**Methodology:** Confluent cultures of rat MSCs were subjected to a biphasic induction protocol, with initial exposure to 1 mM BME for 24 h followed by 10 mM BME for 5 h. Ascorbic acid (AA) served as a positive control, and untreated MSCs as a negative control. Differentiation was assessed based on morphological criteria (soma shape, neurite number and length) using a standardized scoring rubric, and quantified with ImageJ. **Results:** BME-treated MSCs exhibited significant neurogenic morphological features, including soma rounding and extended neurites, with a high proportion scoring in neuronal-like categories. One-way ANOVA with Tukey's post-hoc test revealed significant differences ( $p < 0.0001$ ) in all morphological metrics between treated and untreated groups. While AA induced longer neurites ( $p < 0.01$  vs. BME), no significant difference in the proportion of neuronal-like cells was observed between AA and BME groups ( $p > 0.05$ ). **Conclusion:** These findings suggest that BME is a viable, cost-effective candidate for neurogenic induction protocols and may contribute to the development of simplified, chemically defined strategies for neuronal differentiation in regenerative medicine.

**Keywords:** mesenchymal stem cells, neurogenic differentiation, small molecules,  $\beta$ -mercaptoethanol, neuronal morphology

## INTRODUCTION

Neurodegenerative disorders are characterized by progressive neuronal loss, leading to irreversible deficits in motor and cognitive functions. The limited regenerative capacity of the central nervous system poses a major challenge for therapeutic intervention. Mesenchymal stem cells (MSCs) have emerged as a versatile platform for regenerative medicine due to their self-renewal capacity, multipotency, and immunomodulatory properties [1, 2]. Beyond their mesodermal differentiation potential, MSCs can adopt neurogenic phenotypes under defined conditions, positioning them as a potential source for cell-based therapies in neurological disease [3, 4].

Traditional neurogenic induction protocols often rely on combinations of growth factors, such as basic fibroblast growth factor (bFGF), epidermal growth factor (EGF), and platelet-derived growth factor (PDGF), as well as cytokines and neurotrophins which are expensive and yield inconsistent outcomes [5, 6]. Small molecules offer a simpler, cost-effective alternative. Among them,  $\beta$ -mercaptoethanol (BME) has been reported to induce neuron-like morphology in MSCs, potentially through modulation of redox status and activation of neurogenic transcription factors [7, 8].

This study investigates the ability of BME to induce morphological features associated with neuronal differentiation in bone marrow-derived MSCs, without the use of additional growth factors and other complex chemicals. Ascorbic acid (AA) served as a positive control and untreated cells were used as baseline. The focus on morphological endpoints provides a rapid, non-invasive evaluation method that could support the development of practical neurogenic induction strategies.

## MATERIALS AND METHODS

### Materials

#### Cell Culture

MSCs were isolated from bone marrow of wild type (WT), male Wistar rat, weighing around 200 g, at 7 weeks postnatal age. All procedures involving animal use were conducted in accordance with institutional guidelines and approved by the UNIMAS Animal Ethics Committee (Ref. No: UNIMAS/NC-21.02/09.22(05)).

#### Chemicals, Consumables and Equipment

The chemicals, culture media and consumables used in this study were those currently available in the Biochemistry Lab in the Faculty of Medicine and Health Sciences. The list of chemicals and culture media is in Appendix 2. The equipment used included a biosafety cabinet, CO<sub>2</sub> incubator, phase-contrast microscope, water bath and 4°C refrigerator, all of which were located in the same laboratory. Approval to use the laboratory facilities, consumables, and chemicals had been granted by the lab owner.

### Methods

#### Maintenance of MSCs

Bone marrow aspirate was cultured in pre-coated T25 tissue culture flasks. MSCs were cultured at a density of 250,000/flask, in complete Dulbecco's Modified Eagle's Medium (DMEM) (Thermo Fisher Scientific, Waltham, MA, USA), supplemented with 10% (v/v) fetal bovine serum (Corning, Mediatech, CA, USA), 100 U/mL penicillin, and 0.1 mg/mL streptomycin (Corning, Mediatech, CA, USA), and incubated in a humidified atmosphere with 5% CO<sub>2</sub> at 37°C.

1  
2  
3 Nonadherent hematopoietic cells were removed through frequent medium changes, every other  
4 day. MSCs were subcultured at 80% confluency. Upon reaching passage 2 (P2), nine flasks  
5  
6 containing healthy MSCs that reached 80% confluency were proceeded with treatment.  
7  
8  
9

### 11 12 **Differentiation of MSCs into Neuronal Lineage**

13  
14 Nine flasks containing confluent MSCs were divided into three groups (each group consisted of  
15 three flasks, n = 3 flasks). The three groups were 1) No treatment 2) Ascorbic Acid (AA) treatment  
16  
17 (Thermo Fisher Scientific, Waltham, MA, USA), and 3)  $\beta$ -mercaptoethanol (BME) treatment  
18  
19 (AMRESCO, Ohio, USA).  
20  
21  
22  
23  
24  
25

### 26 **Initial Treatment**

27  
28 MSCs for group 2 and group 3 were initially treated with 50  $\mu$ M AA and 1 mM BME respectively,  
29  
30 each diluted in complete culture media within individual flasks for the first 24 hours as biphasic  
31  
32 treatment.  
33  
34  
35  
36  
37

### 38 **Subsequent Treatments**

39  
40 Following an overnight incubation, the media was replaced with fresh serum-free media containing  
41  
42 200  $\mu$ M AA for MSCs in group A, and 10 mM BME for MSCs in group B, incubated for another  
43  
44 3 hours. After 3 hours, MSCs in both groups were quenched with fresh complete media and  
45  
46 monitored under phase-contrast microscope to observe for morphological observations.  
47  
48  
49  
50  
51  
52  
53  
54  
55  
56  
57  
58  
59  
60

## Morphological Assessment and Image Acquisition

High-resolution images were taken at 10x or 20x magnification to create a visual record of the differentiation process. From each flask, five non-overlapping images were captured, yielding a total of 15 images per group.

## Differentiation Scoring Rubric and Decision Tree

MSCs were assessed for neuronal morphology based on predefined criteria using a morphological scoring rubric. Only cells scoring 2 or 3 were considered to be differentiated into neuronal-like cells and included in the quantification of differentiation. The rubric is shown in **Table 1**. A decision tree was followed to guide scoring. This is shown in **Figure 1**.

## Quantification of Differentiated Cells

For each image:

- Total cells were counted manually using ImageJ's Cell Counter plugin.
- Each cell was scored using rubric.
- The number of cells with a score of 2 or 3 was recorded.

Differentiated cells were then counted using the formula in **Figure 1**. For each flask, the percentage values from five images were averaged to yield one biological replicate. The resulting values (n = 3 per group) were used for statistical analysis. These values were then used to analyze:

- Percentage of differentiated MSCs into neuronal lineage across the three groups
- Percentage of highly neuronal-like cells
- Percentage of neuronal-like cells

### **Raw Count Analysis of Differentiated vs. Undifferentiated Cells**

In addition to calculating the percentage of differentiated cells, the absolute number of differentiated versus undifferentiated MSCs was also quantified across all treatment groups. Using the same morphological scoring rubric and decision tree, each cell within every image was manually categorized as either neuronal-like (Score 2 or 3) or undifferentiated (Score 0 or 1). Raw counts for each category were recorded for all 15 images per group (5 images  $\times$  3 flasks), without converting the data into percentages. The total number of differentiated cells (Score 2+3) and undifferentiated cells (Score 0+1) per group was compiled and used for further comparative analysis. These counts provided a complementary view of group-wise differences in differentiation response, independent of field size or percentage normalization.

### **Neurite Length Measurement**

Neurite length was quantified to further assess the degree of neuronal-like differentiation in MSCs. For each group, five representative neuronal-like cells (with clear neurite projections) were randomly selected across the captured fields, resulting in a total of 5 measurements per group. ImageJ (Fiji distribution) was used for all neurite measurements. Prior to analysis, the image scale was calibrated by setting the known pixel-to-micrometer ratio based on the 10 $\times$  magnification objective (1 pixel  $\approx$  1.1  $\mu$ m). The segmented line tool was used to manually trace the length of each neurite, from the edge of the soma to the tip of the projection. All neurites in a cell were measured, and care was taken to exclude overlapping or unclear projections. The measured neurite lengths (in  $\mu$ m) were recorded for each cell, and the mean neurite length was calculated per group.

### Statistical Analysis

All data were analyzed using Data Analysis function in Microsoft Excel and GraphPad Prism. Differences in mean percentage of neuronal-like cells, highly neuronal-like cells, differentiated cells across all groups, raw count analysis, and neurite length were assessed using one-way ANOVA followed by Tukey's post-hoc test. Data were presented as mean  $\pm$  standard error mean (SEM), and a p-value of  $< 0.05$  was considered statistically significant.

For Review Only

## RESULTS

### Morphological Changes

MSCs represent non-hematopoietic subpopulation of the bone marrow. These cells displayed a stable phenotype of monolayer cultures. Untreated MSCs retained a fibroblast-like morphology with elongated cell bodies and no neurite projections (**Figure 2**). In contrast, both AA- and BME-treated cells developed rounded cell body with thin, elongated neurites which are more widely distributed (**Figure 3 & 4, respectively**). BME-treated cultures displayed frequent multipolar morphologies with interconnected processes, indicative of early neuronal differentiation.

### Differentiation Rates

#### Percentage of Differentiated Cells

Based on the morphological scoring rubric (**Table 1**), the status of cell differentiations was determined and compared between the three groups of MSCs. The proportion of MSCs that adopted a neuronal-like morphology differed significantly across groups (**Figure 5; Supplementary Table S1**). Untreated MSCs showed minimal spontaneous differentiation, with only  $1.36 \pm 0.42\%$  of cells meeting the morphological criteria for neuronal-like phenotypes. In contrast, both treatment groups demonstrated markedly higher differentiation percentages, with  $92.88 \pm 2.41\%$  in the AA group and  $90.53 \pm 1.73\%$  in the BME group ( $p < 0.0001$  vs. untreated). No significant difference was observed between AA- and BME-treated groups ( $p > 0.05$ ).

#### Percentage of Highly Neuronal-Like Cells

Cells classified as highly neuronal-like exhibited refracted soma, bipolar or multipolar morphology, and the presence of more than two branching neurites (**Figure 6; Supplementary Table S2**). A negligible percentage ( $0.13 \pm 0.08\%$ ) of untreated MSCs fell into this category,

1  
2  
3 compared to  $84.93 \pm 3.64\%$  in the BME group and  $82.27 \pm 2.73\%$  in the AA group. Both treated  
4  
5 groups showed statistically significant increases over untreated controls ( $p < 0.0001$ ), while no  
6  
7 difference was observed between AA and BME groups.  
8  
9

### 11 12 **Percentage of Neuronal-Like Cells**

13  
14 When assessing cells with rounded somata and at least one long neurite projection, untreated MSCs  
15  
16 displayed a low differentiation percentage of  $1.23 \pm 0.42\%$  (**Figure 7; Supplementary Table S3**).  
17  
18 In contrast, the BME and AA groups demonstrated significantly elevated proportions, at  $8.26 \pm$   
19  
20  $1.60\%$  and  $7.95 \pm 1.37\%$ , respectively ( $p < 0.05$  vs. untreated). These results suggest that both  
21  
22 small molecules not only increased the overall number of differentiated cells but also promoted  
23  
24 acquisition of neuronal-like phenotypes.  
25  
26  
27  
28  
29

### 30 31 **Percentage of Differentiated vs. Undifferentiated Cells**

32  
33 Pie chart analysis further illustrated the stark contrast between untreated and treated groups  
34  
35 (**Figures 8-10**). In the absence of chemical inducers, 98.1% of MSCs remained undifferentiated,  
36  
37 with only 1.9% adopting neuronal-like features. Treatment with AA reduced the proportion of  
38  
39 undifferentiated cells to 5.21%, with 94.79% undergoing differentiation. Similarly, the BME group  
40  
41 exhibited 90.98% differentiated cells, leaving only 9.02% undifferentiated. These findings  
42  
43 underscore the effectiveness of small molecules in significantly shifting the balance toward  
44  
45 neuronal-like phenotypes.  
46  
47  
48  
49

### 50 51 **Mean of Neurite Length**

52  
53 Neurite length was employed as a quantitative measure of neuronal maturation (**Figure 11;**  
54  
55 **Supplementary Table S4**). Untreated MSCs displayed only minimal outgrowth, with a mean  
56  
57  
58  
59  
60

1  
2  
3 neurite length of  $133.80 \pm 35.60 \mu\text{m}$ . Both AA- and BME-treated cells exhibited significantly  
4 longer neurites, measuring  $409.50 \pm 26.19 \mu\text{m}$  and  $288.70 \pm 25.48 \mu\text{m}$ , respectively ( $p < 0.0001$   
5 vs. untreated). AA-treated cells demonstrated significantly longer neurites than BME-treated cells  
6 ( $p < 0.01$ ), suggesting a superior effect of AA in promoting neurite extension.  
7  
8  
9  
10  
11  
12  
13  
14  
15  
16  
17  
18  
19  
20  
21  
22  
23  
24  
25  
26  
27  
28  
29  
30  
31  
32  
33  
34  
35  
36  
37  
38  
39  
40  
41  
42  
43  
44  
45  
46  
47  
48  
49  
50  
51  
52  
53  
54  
55  
56  
57  
58  
59  
60

For Review Only

## DISCUSSION

This study evaluated the neurogenic differentiation potential of mesenchymal stem cells (MSCs) following treatment with  $\beta$ -mercaptoethanol (BME), small-molecule inducer, with particular focus on morphological changes and neurite outgrowth. The results revealed that MSCs exposed to chemical induction underwent marked transformations, shifting from a fibroblast-like morphology to rounded, neuron-like cells with extended processes resembling axons and dendrites. Quantitative analyses confirmed that the proportion of differentiated and highly neuronal-like cells was significantly greater in treated groups (BME- and AA-treated) compared to untreated controls. These findings underline the capacity of small molecules to serve as effective and accessible tools for inducing neuronal-like characteristics in MSCs.

A central outcome of this work is the demonstration that a single small-molecule induction can replicate morphological changes typically achieved using growth factor-enriched protocols. The acquisition of refracted soma, elongated neurites, and multipolar branching reflects hallmark features of neuronal commitment. Similar observations have been reported in previous studies where small molecules were shown to promote neurogenic differentiation across different MSC sources, including bone marrow and adipose tissue [8, 9]. Importantly, in the present study, these outcomes were achieved without supplementation with exogenous growth factors such as EGF, bFGF or PDGF, as well as cytokines and neurotrophins underscoring the simplicity and cost-effectiveness of this approach. This finding strengthens the evidence that small molecules can act independently to activate intrinsic neurogenic pathways, possibly through redox modulation and signaling cascades such as PI3K/Akt or Wnt/ $\beta$ -catenin [10, 11].

1  
2  
3 The comparative analysis between ascorbic acid (AA), a well-established neurogenic inducer, and  
4 BME further highlights the translational value of this approach. Both compounds significantly  
5 increased the percentage of differentiated cells to over 90%, with no statistically significant  
6 difference between the two treatments. While AA-treated cells displayed slightly longer neurites,  
7 the ability of BME to produce comparable proportions of neuronal-like cells suggests that it may  
8 represent an equally effective yet more cost-efficient option. The high reproducibility across  
9 biological replicates, reflected in low standard error values, also enhances confidence in the  
10 robustness of this induction strategy.  
11  
12  
13  
14  
15  
16  
17  
18  
19  
20  
21  
22  
23

24 The presence of highly neuronal-like cells in both treatment groups, characterized by multipolar  
25 morphology and extensive branching, is particularly noteworthy. These features suggest advanced  
26 progression toward neuronal phenotypes and potential readiness for functional maturation.  
27 Although this study relied primarily on morphological criteria, such complexity in cellular  
28 architecture is often associated with early synaptic organization and network formation [7]. Thus,  
29 while functional validation remains a future requirement, the morphological evidence strongly  
30 supports the neuro-inductive potential of small molecules.  
31  
32  
33  
34  
35  
36  
37  
38  
39  
40  
41

42 Despite these promising outcomes, several limitations must be acknowledged. First, the study did  
43 not incorporate molecular confirmation of neuronal identity through markers such as  $\beta$ III-tubulin,  
44 MAP2, or NeuN. Morphological criteria, although useful as early indicators, cannot fully verify  
45 lineage specificity. Second, the short observation period of 29 hours precluded assessment of long-  
46 term stability, maturation, and survival of the differentiated cells. Third, functional assays such as  
47 patch-clamp electrophysiology or calcium imaging were not performed, leaving unanswered  
48  
49  
50  
51  
52  
53  
54  
55  
56  
57  
58  
59  
60

1  
2  
3 whether the neuron-like cells exhibited electrophysiological properties or synaptic activity.  
4  
5 Finally, the study employed MSCs from a single rat bone marrow source, which may limit the  
6  
7 generalizability of the results across species or tissue origins.  
8  
9

10  
11  
12 Future studies should therefore incorporate molecular and immunocytochemical analyses to verify  
13  
14 neuronal lineage commitment, extend observation periods to monitor long-term maturation, and  
15  
16 perform functional assays to assess electrophysiological competency. Expanding the work to  
17  
18 include MSCs from diverse sources and donors, as well as in vivo models of neurodegenerative  
19  
20 disease, would provide essential insights into the survival, integration, and functional recovery  
21  
22 potential of induced neuron-like cells. Such validation will be crucial for translating these findings  
23  
24 into clinically relevant applications.  
25  
26  
27  
28  
29

### 30 31 **CONCLUSION**

32  
33 This study provides compelling evidence that a single small-molecule inducer can promote  
34  
35 neurogenic differentiation of MSCs, producing morphological outcomes comparable to those  
36  
37 achieved with established inducers like ascorbic acid. The results highlight the feasibility of using  
38  
39 chemically defined, low-cost, and accessible methods to generate neuronal-like cells, offering  
40  
41 practical advantages over complex chemical and growth factor-based protocols. While further  
42  
43 molecular and functional validation is needed, the findings reinforce the potential of small  
44  
45 molecules as valuable tools in regenerative medicine and as promising candidates for the  
46  
47 development of simplified neurogenic protocols aimed at treating neurodegenerative disorders.  
48  
49  
50  
51  
52  
53  
54  
55  
56  
57  
58  
59  
60

## REFERENCES

1. Zakrzewski W, Dobrzyński M, Szymonowicz M, Rybak Z. Stem cells: past, present, and future. *Stem Cell Research & Therapy*. 2019 Feb 26;10(1). <https://doi.org/10.1186/s13287-019-1165-5>
2. Vizoso FJ, Costa LA, Eiro N. New era of mesenchymal stem cell-based medicine: basis, challenges and prospects. *Revista Clínica Española (English Edition)*. 2023 Nov 23;223(10):619–28. <https://doi.org/10.1016/j.rceng.2023.11.002>
3. Tong LM, Fong H, Huang Y. Stem cell therapy for Alzheimer's disease and related disorders: current status and future perspectives. *Experimental & Molecular Medicine*. 2015 Mar 13;47(3):e151. <https://doi.org/10.1038/emm.2014.124>
4. Margiana R, Markov A, Zekiy AO, Hamza MU, Al-Dabbagh KA, Al-Zubaidi SH, et al. Clinical application of mesenchymal stem cell in regenerative medicine: a narrative review. *Stem Cell Research & Therapy*. 2022 Jul 28;13(1). <https://doi.org/10.1186/s13287-022-03054-0>
5. Liu F, Xuan A, Chen Y, Zhang J, Xu L, Yan Q, et al. Combined effect of nerve growth factor and brain-derived neurotrophic factor on neuronal differentiation of neural stem cells and the potential molecular mechanisms. *Molecular Medicine Reports*. 2014 Jul 18;10(4):1739–45. <https://doi.org/10.3892/mmr.2014.2393>
6. Skaper SD. Neurotrophic Factors: An Overview. *Methods in Molecular Biology*. 2017 Dec 8;1–17. [https://doi.org/10.1007/978-1-4939-7571-6\\_1](https://doi.org/10.1007/978-1-4939-7571-6_1)
7. Mohan G, Shamsuddin AA, Adli DH, Moghadamtousi SZ, Khanabdali R, Saadat A, et al. Promoting effect of small molecules in cardiomyogenic and neurogenic differentiation of rat bone marrow-derived mesenchymal stem cells. *Drug Design Development and Therapy*. 2015 Dec 1;81. <https://doi.org/10.2147/dddt.s89658>
8. Mohammad M, Al-Shammari AM, Abdulla RH, Ahmed A, Khalid A. Differentiation of Adipose-Derived Mesenchymal Stem Cells into Neuron-Like Cells induced by using  $\beta$ -mercaptoethanol. *Baghdad Science Journal*. 2020 Mar 18;17(1(Suppl.)):0235. [https://doi.org/10.21123/bsj.2020.17.1\(suppl.\).0235](https://doi.org/10.21123/bsj.2020.17.1(suppl.).0235)
9. Park J, Lee N, Lee J, Choe EK, Kim MK, Lee J, et al. Small molecule-based lineage switch of human adipose-derived stem cells into neural stem cells and functional GABAergic neurons. *Scientific Reports*. 2017 Aug 25;7(1). <https://doi.org/10.1038/s41598-017-10394-y>
10. Kamali A, Ziadlou R, Lang G, Pfannkuche J, Cui S, Li Z, et al. Small molecule-based treatment approaches for intervertebral disc degeneration: Current options and future directions. *Theranostics*. 2020 Oct 9;11(1):27–47. <https://doi.org/10.7150/thno.48987>
11. Oliveira LFS, Predes D, Borges HL, Abreu JG. Therapeutic potential of naturally occurring small molecules to target the WNT/B-Catenin signaling pathway in colorectal cancer. *Cancers*. 2022 Jan 14;14(2):403. <https://doi.org/10.3390/cancers14020403>
12. Urrutia DN, Caviedes P, Mardones R, Minguell JJ, Vega-Letter AM, Jofre CM. Comparative study of the neural differentiation capacity of mesenchymal stromal cells from different tissue sources: An approach for their use in neural regeneration therapies. *PLoS ONE*. 2019 Mar 11;14(3):e0213032. <https://doi.org/10.1371/journal.pone.0213032>

## Table Legend

**Table 1.** Morphological scoring rubric, adapted based on neuronal-like features observed during mesenchymal stem cell differentiation [12].

## Figure Legends

**Fig. 1.** Decision tree for classification of MSCs post-treatment, based on neuronal-like morphology. Cells were first assessed for soma shape and the presence of neurite-like extensions. A cell with a rounded soma and at least one long process was classified as “neuronal-like” (Score 2). Cells exhibiting two or more processes were classified as “highly neuronal-like” (Score 3). Only cells with a score of 2 or 3 were included in the quantification of neuronal differentiation. Flat/Spindle/Short characteristics are regarded as “undifferentiated” or “transitional”.

**Fig. 2.** Morphological characteristics of untreated MSCs. (A) and (B) show untreated MSCs with spindle-shaped morphology and clonal properties from two representative fields.

**Fig. 3.** Morphological changes in MSCs treated with AA. (A), (B), (C), and (D) show MSCs with rounded cell bodies with visible multipolar dendrites. Interconnecting networks can be seen with neighbouring cells, indicating neuron-like cellular morphology.

**Fig. 4.** Morphological changes in MSCs treated with BME. (A), (B), (C), and (D) display MSCs exhibiting rounded somas with clear sprouting dendrite-like projections. The presence of interconnected networks between adjacent cells forming axons and dendrites further supports their neuron-like morphological characteristics.

**Fig. 5.** Quantitative analysis of differentiated MSCs following treatment with ascorbic acid (AA),  $\beta$ -mercaptoethanol (BME), or no treatment. Both AA- and BME-treated groups exhibited significantly higher proportions of differentiated cells compared to untreated controls ( $p < 0.0001$ ). Data are presented as mean  $\pm$  SEM ( $n = 3$ ).

**Fig. 6.** Quantitative analysis of highly neuronal-like MSCs, characterized by multipolar morphology with  $\geq 2$  neurites, after treatment with AA, BME, or no treatment. Both AA- and BME-treated groups demonstrated significantly higher percentages of highly neuronal-like cells than untreated controls ( $p < 0.0001$ ). Data are presented as mean  $\pm$  SEM ( $n = 3$ ).

**Fig. 7.** Quantitative analysis of neuronal-like MSCs, defined as cells with rounded somata and at least one long neurite, following treatment with AA, BME, or no treatment. Both treated groups showed significantly greater neuronal-like differentiation compared to untreated MSCs ( $p < 0.05$ ). Data are presented as mean  $\pm$  SEM ( $n = 3$ ).

**Fig. 8.** Pie chart showing the distribution of differentiated vs. undifferentiated MSCs in the untreated group. The majority of cells (98.1%) remained undifferentiated, with only 1.9% displaying neuronal-like morphology.

1  
2  
3 **Fig. 9.** Pie chart showing the distribution of differentiated vs. undifferentiated MSCs in the AA-  
4 treated group. A total of 94.79% of MSCs underwent differentiation into neuronal-like phenotypes,  
5 while 5.21% remained undifferentiated.  
6

7  
8 **Fig. 10.** Pie chart showing the distribution of differentiated vs. undifferentiated MSCs in the BME-  
9 treated group. Differentiation occurred in 90.98% of cells, whereas 9.02% remained  
10 undifferentiated.  
11

12 **Fig. 11.** Mean neurite length of MSCs following treatment with AA, BME, or no treatment. Both  
13 AA and BME significantly increased neurite outgrowth compared to untreated controls ( $p <$   
14  $0.0001$ ). AA treatment induced significantly longer neurites compared to BME ( $p < 0.01$ ). Data  
15 are presented as mean  $\pm$  SEM ( $n = 3$ ).  
16  
17  
18  
19  
20  
21  
22  
23  
24  
25  
26  
27  
28  
29  
30  
31  
32  
33  
34  
35  
36  
37  
38  
39  
40  
41  
42  
43  
44  
45  
46  
47  
48  
49  
50  
51  
52  
53  
54  
55  
56  
57  
58  
59  
60

1  
2  
3  
4  
5  
6  
7  
8  
9  
10  
11  
12  
13  
14  
15  
16  
17  
18  
19  
20  
21  
22  
23  
24  
25  
26  
27  
28  
29  
30  
31  
32  
33  
34  
35  
36  
37  
38  
39  
40  
41  
42  
43  
44  
45  
46  
47  
48  
49  
50  
51  
52  
53  
54  
55  
56  
57  
58  
59  
60

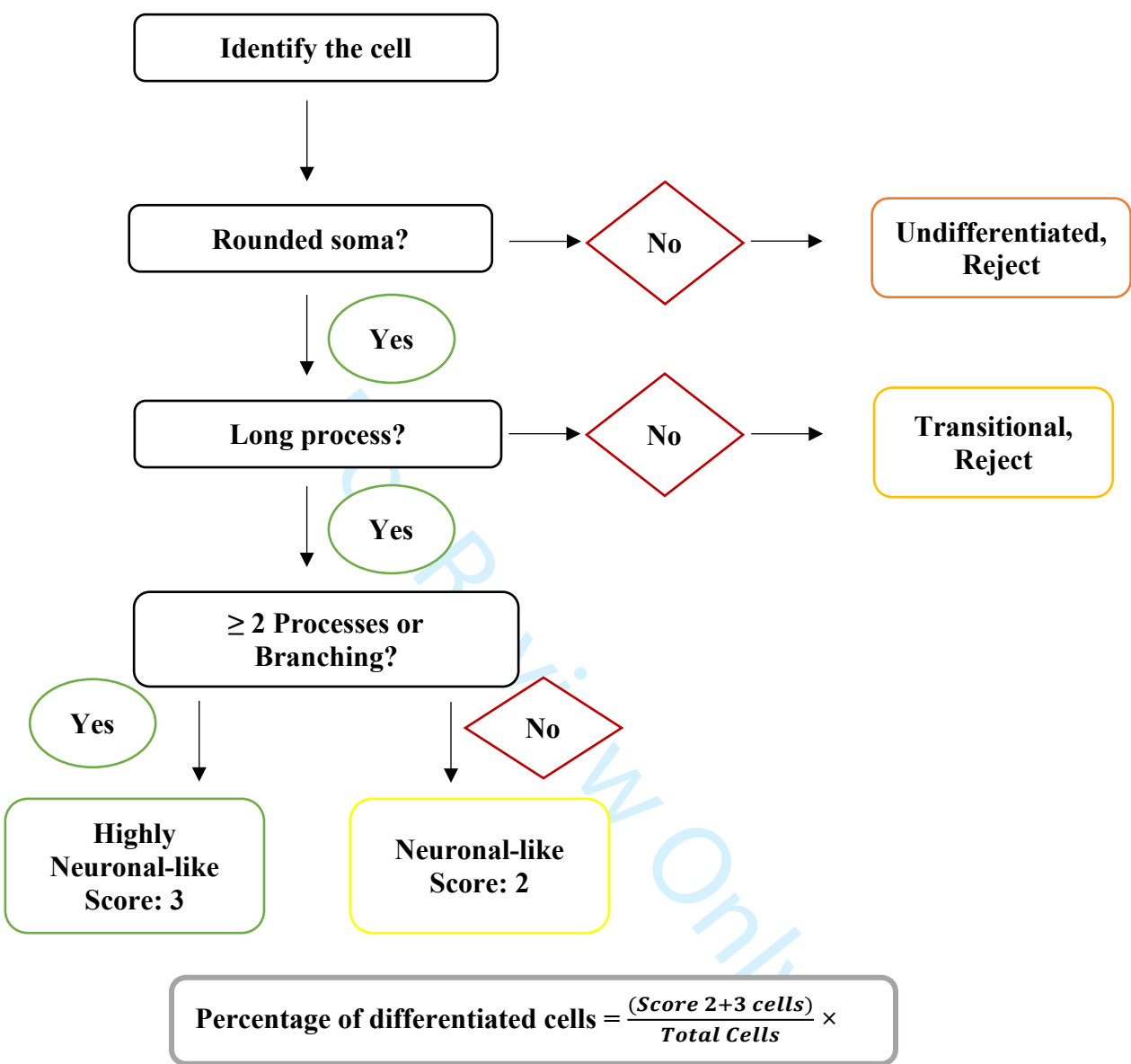
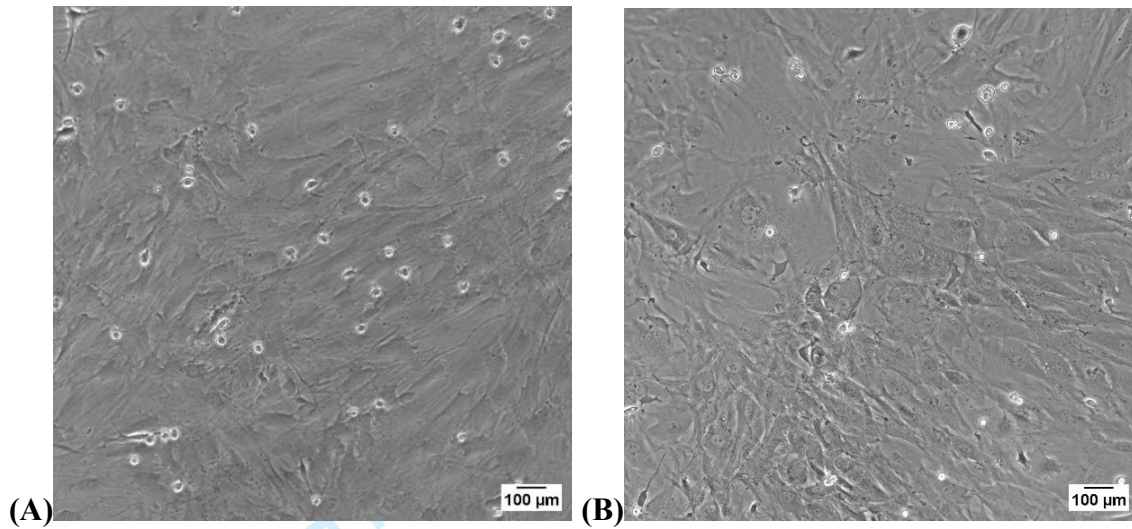
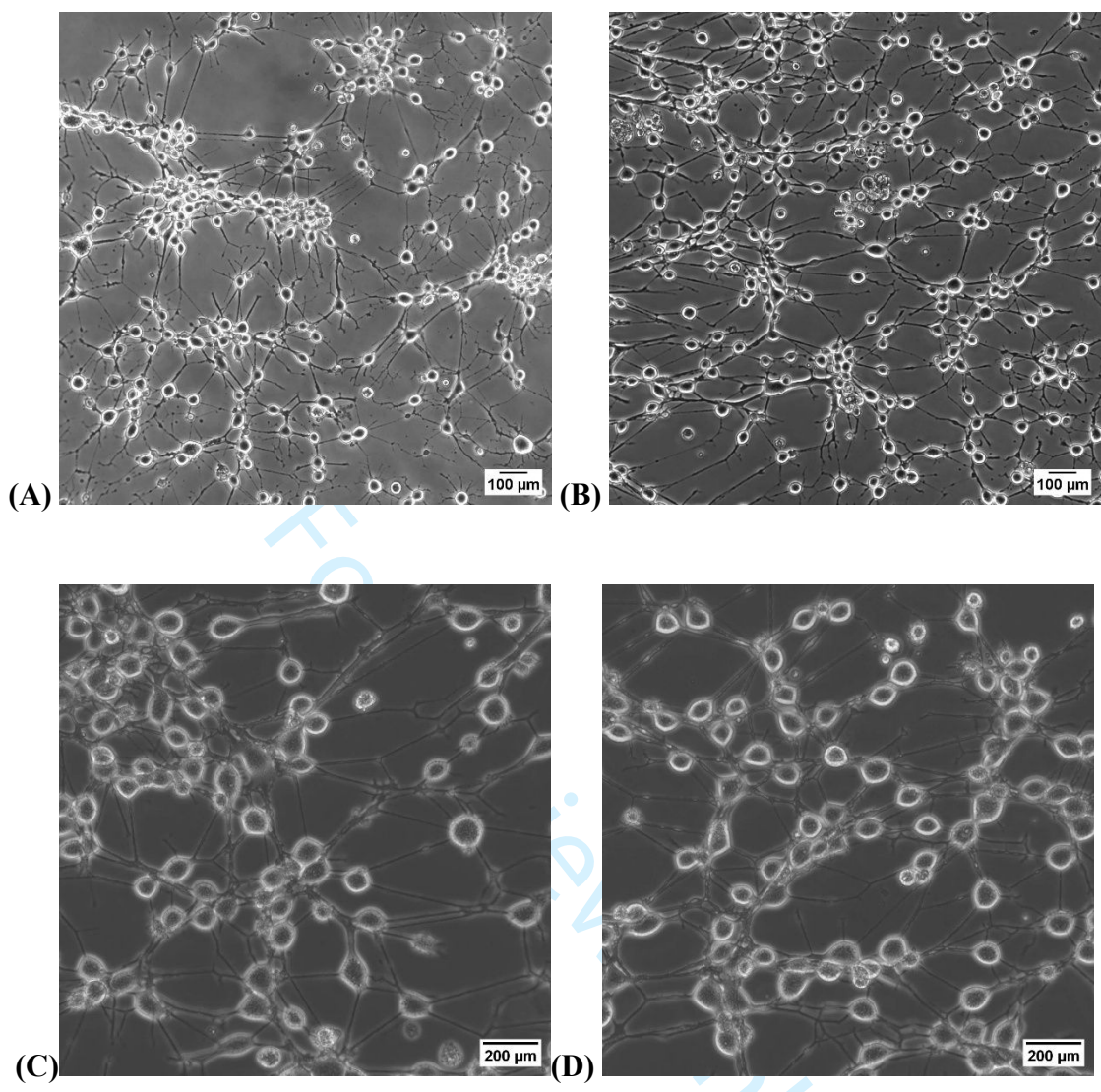


Fig. 1.



**Fig. 2.**

1  
2  
3  
4  
5  
6  
7  
8  
9  
10  
11  
12  
13  
14  
15  
16  
17  
18  
19  
20  
21  
22  
23  
24  
25  
26  
27  
28  
29  
30  
31  
32  
33  
34  
35  
36  
37  
38  
39  
40  
41  
42  
43  
44  
45  
46  
47  
48  
49  
50  
51  
52  
53  
54  
55  
56  
57  
58  
59  
60



**Fig. 3. MSCs treated with AA.**

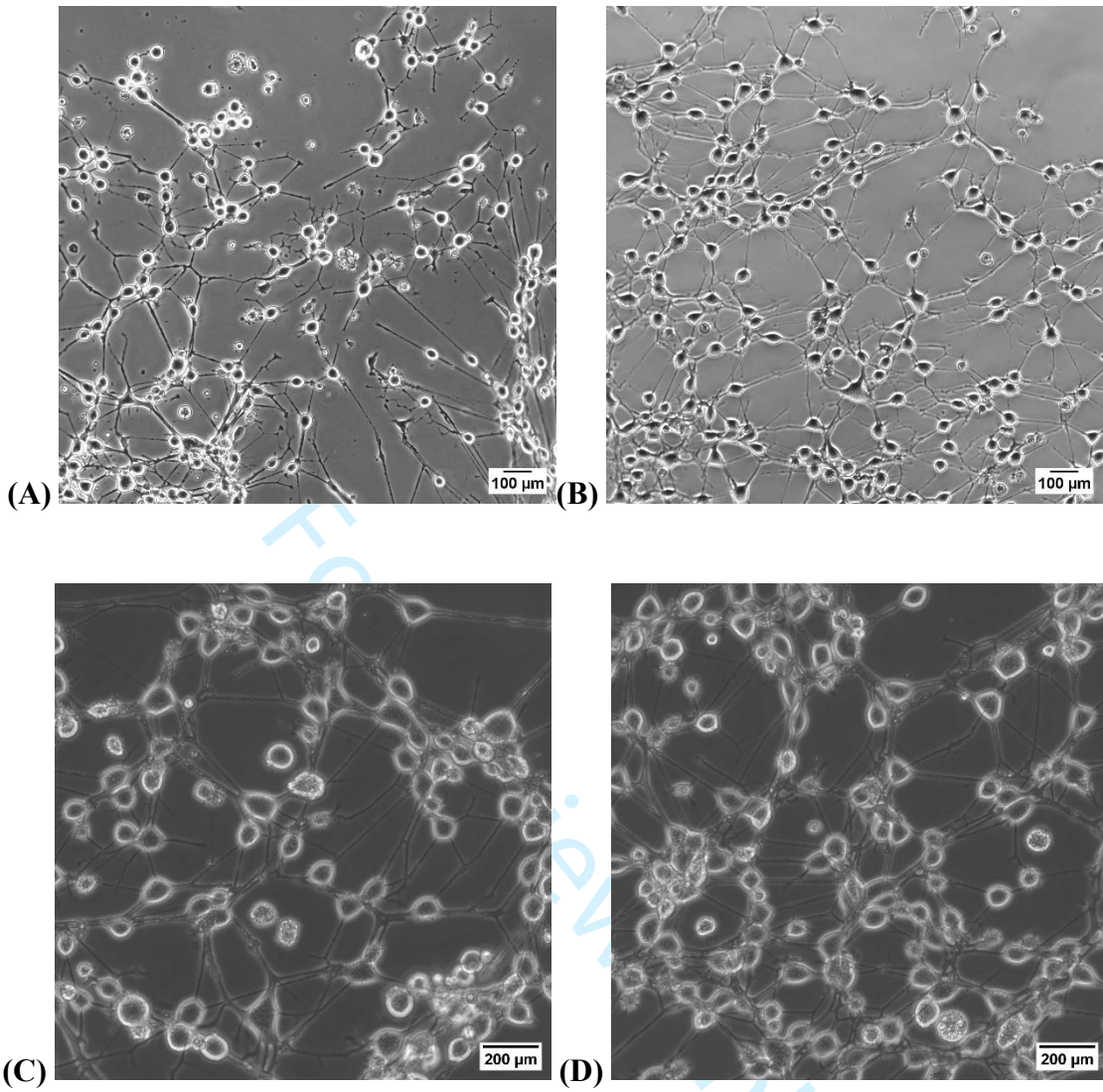


**Fig. 4. MSCs treated with BME.**

1  
2  
3  
4  
5  
6  
7  
8  
9  
10  
11  
12  
13  
14  
15  
16  
17  
18  
19  
20  
21  
22  
23  
24  
25  
26  
27  
28  
29  
30  
31  
32  
33  
34  
35  
36  
37  
38  
39  
40  
41  
42  
43  
44  
45  
46  
47  
48  
49  
50  
51  
52  
53  
54  
55  
56  
57  
58  
59  
60

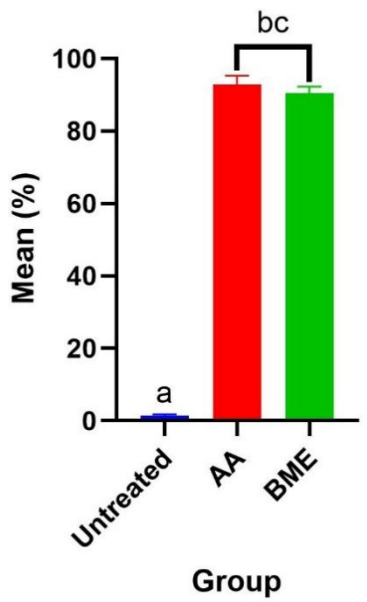


Fig. 5.

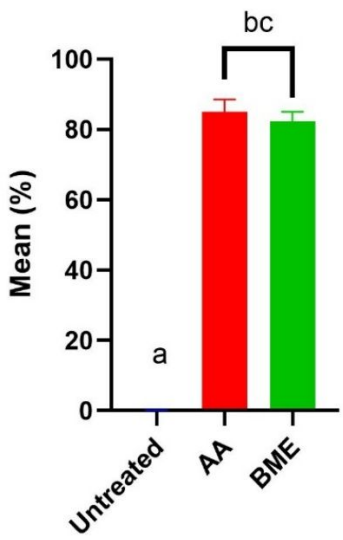


Fig. 6.

For Review Only

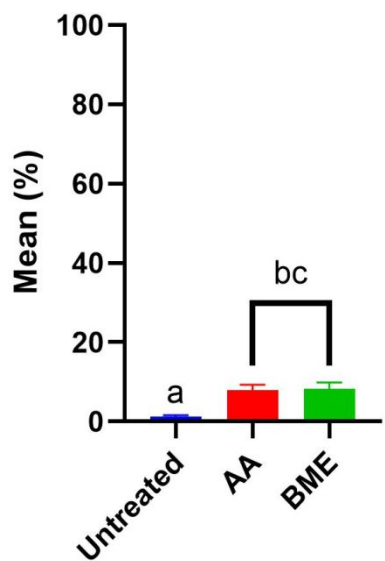


Fig. 7.

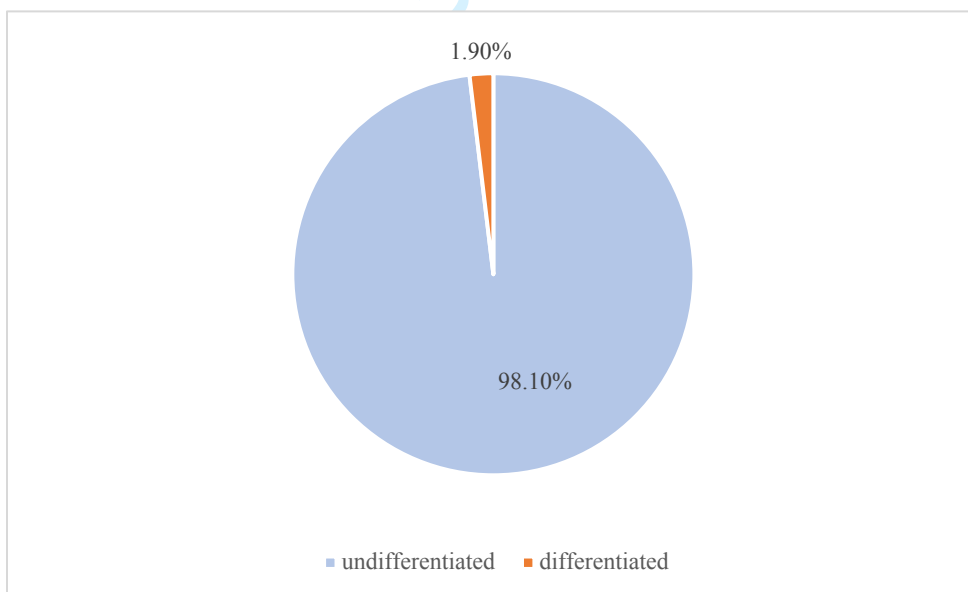
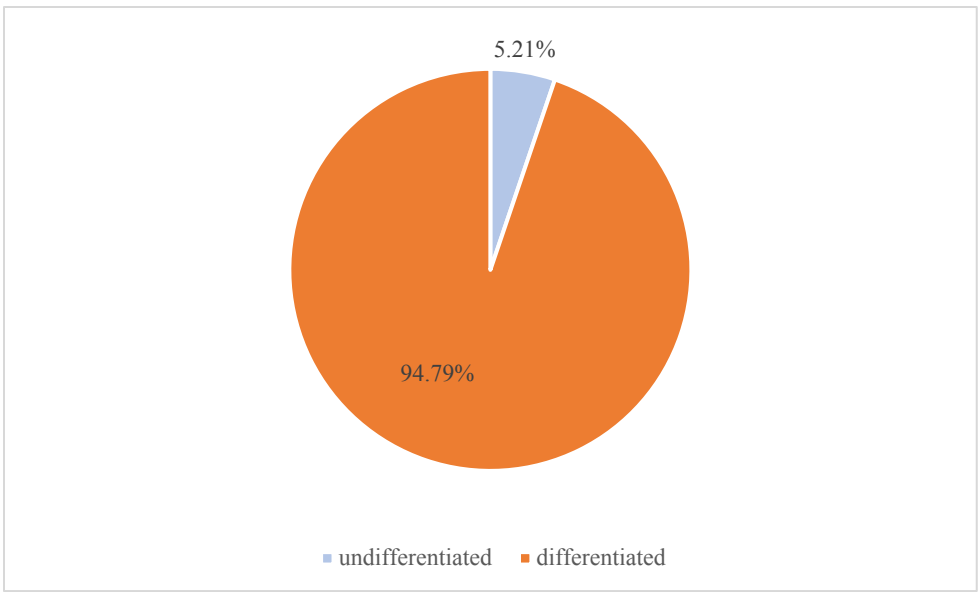
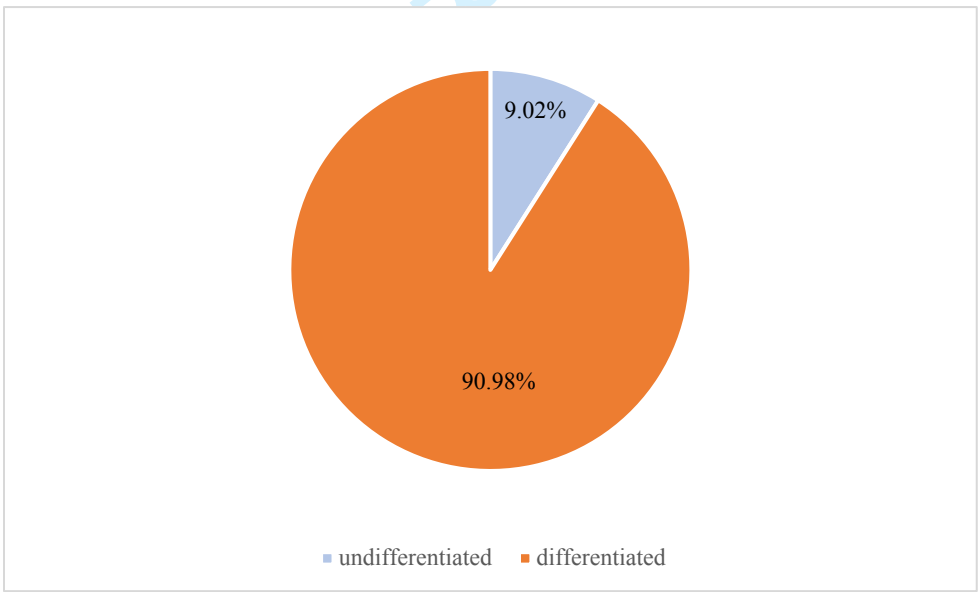


Fig. 8.

1  
2  
3  
4  
5  
6  
7  
8  
9  
10  
11  
12  
13  
14  
15  
16  
17  
18  
19  
20  
21  
22  
23  
24  
25  
26  
27  
28  
29  
30  
31  
32  
33  
34  
35  
36  
37  
38  
39  
40  
41  
42  
43  
44  
45  
46  
47  
48  
49  
50  
51  
52  
53  
54  
55  
56  
57  
58  
59  
60



**Fig. 9.**



**Fig. 10.**

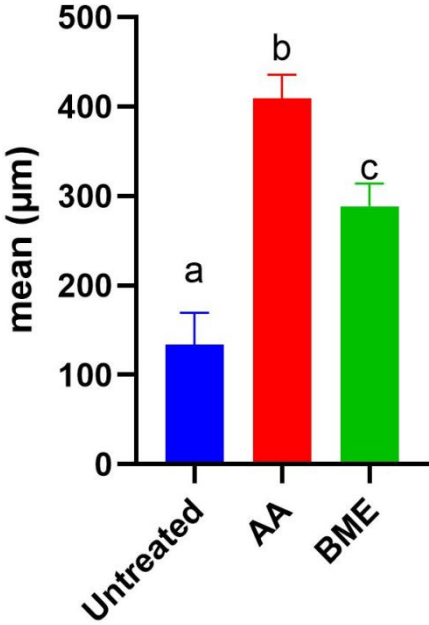


Fig. 11.

Review Only

**Table 1.**

<b>Score</b>	<b>Cell Morphology</b>	<b>Description</b>
<b>0</b>	Undifferentiated	Flat, spindle-shaped or fibroblast-like morphology; no neurite extensions
<b>1</b>	Transitional	Slightly rounded soma; short, thick protrusion; early signs of elongations
<b>2</b>	Neuronal-like	Rounded soma; 1 long process, thin neurite-like projection
<b>3</b>	Highly Neuronal-Like	Rounded soma; visible bipolar/multipolar shape; $\geq 2$ neurites with branching or tapering

For Review Only

The following supplementary data are provided to support the quantitative findings presented in the main text. While the figures in the Results section summarize the overall trends, these tables present the detailed descriptive statistics and post-hoc analyses for transparency and reproducibility.

**Supplementary Table S1.** Percentage of differentiated MSCs across treatment groups.

Values are presented as mean  $\pm$  SEM (n = 3). Different superscript letters (a, b and c) indicate significant differences between groups (one-way ANOVA with Tukey's post-hoc test,  $p < 0.05$ ).

Group	Mean (%) $\pm$ SEM
Untreated	1.36 $\pm$ 0.42 <sup>a</sup>
AA	92.88 $\pm$ 2.41 <sup>bc</sup>
BME	90.53 $\pm$ 1.73 <sup>bc</sup>

**Supplementary Table S2.** Percentage of highly neuronal-like MSCs across treatment groups.

Values are presented as mean  $\pm$  SEM (n = 3). Different superscript letters (a, b and c) indicate significant differences between groups (one-way ANOVA with Tukey's post-hoc test,  $p < 0.05$ ).

Group	Mean (%) $\pm$ SEM
Untreated	0.13 $\pm$ 0.08 <sup>a</sup>
AA	84.93 $\pm$ 3.64 <sup>bc</sup>
BME	82.27 $\pm$ 2.73 <sup>bc</sup>

**Supplementary Table S3.** Percentage of neuronal-like MSCs across treatment groups. Values are presented as mean  $\pm$  SEM (n = 3). Different superscript letters (a, b and c) indicate significant differences between groups (one-way ANOVA with Tukey's post-hoc test,  $p < 0.05$ ).

Group	Mean (%) $\pm$ SEM
Untreated	1.23 $\pm$ 0.42 <sup>a</sup>
AA	7.95 $\pm$ 1.37 <sup>bc</sup>
BME	8.26 $\pm$ 1.60 <sup>bc</sup>

**Supplementary Table S4.** Mean neurite length ( $\mu\text{m}$ ) of MSCs across treatment groups. Values are presented as mean  $\pm$  SEM ( $n = 3$ ). Different superscript letters (a, b and c) indicate significant differences between groups (one-way ANOVA with Tukey's post-hoc test,  $p < 0.05$ ).

<b>Group</b>	<b>Mean (<math>\mu\text{m}</math>) <math>\pm</math> SEM</b>
Untreated	133.80 $\pm$ 35.60 <sup>a</sup>
AA	409.50 $\pm$ 26.19 <sup>b</sup>
BME	288.70 $\pm$ 25.48 <sup>c</sup>

For Review Only